

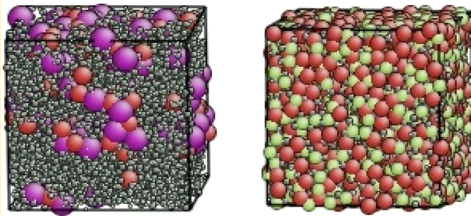
On the Structure of Aqueous Cesium Fluoride and Cesium Iodide Solutions: Diffraction Experiments, Molecular Dynamics Simulations, and Reverse Monte Carlo Modeling

Viktória Mile,[†] Orsolya Gereben,[†] Shinji Kohara,[‡] and László Pusztai^{*,†}

[†]Institute for Solid State Physics and Optics, Wigner Research Centre for Physics, Hungarian Academy of Sciences, P.O. Box 49, H-1525 Budapest, Hungary

[‡]Japan Synchrotron Radiation Research Institute (SPring-8/JASRI), 1-1-1 Kouto, Sayo-cho, Sayo-gun, Hyogo 679-5198, Japan

ABSTRACT: A detailed study of the microscopic structure of two electrolyte solutions, cesium fluoride (CsF) and cesium iodide (CsI) in water, is presented. For revealing the influence of salt concentration on the structure, CsF solutions at concentrations of 15.1 and 32.3 mol % and CsI solutions at concentrations of 1.0 and 3.9 mol % are investigated. For each concentration, we combine total scattering structure factors from neutron and X-ray diffraction and 10 partial radial distribution functions from molecular dynamics simulations in one single structural model, generated by reverse Monte Carlo modeling. For the present solutions we show that the level of consistency between simulations that use simple pair potentials and experimental structure factors is at least semiquantitative for even the extremely highly concentrated CsF solutions. Remaining inconsistencies seem to be caused primarily by water–water distribution functions, whereas slightly problematic parts appear on the ion–oxygen partials, too. As a final result, we obtained particle configurations from reverse Monte Carlo modeling that were in quantitative agreement with both sets of diffraction data and most of the MD simulated partial radial distribution functions. From the particle coordinates, distributions of the number of first neighbors as well as angular correlation functions were calculated. The average number of water molecules around cations in both materials decreases from about 8.0 to about 5.1 as concentration increases, whereas the same quantity for the anions (X) changes from about 5.3 to about 3.7 in the case of CsF and from about 6.2 to about 4.0 in the case of CsI . The average angle of $X\cdots\text{H}\cdots\text{O}$ particle arrangements, characteristic of anion–water hydrogen bonds, is closer to 180° than that found for $\text{O}\cdots\text{H}\cdots\text{O}$ arrangements (water–water hydrogen bonds) at higher concentrations.



1. INTRODUCTION

Despite huge efforts for understanding various properties of electrolyte solutions over the past four decades,¹ they are still challenging from the point of view of their microscopic structure. The main difficulty concerning diffraction measurements is that even the simplest such solution contains four different scattering centers (anion, cation, oxygen, hydrogen). That is, for determining the full set (i.e., 10) of partial radial distribution functions (prdf) one would need 10 independent experimental total scattering structure factors (tssf)—which requirement will never be fulfilled in practice. Computer simulation methods,² on the other hand, can provide detailed description of the structure; unfortunately, here one has to deal with the problem of choosing appropriate interaction potentials.^{1,2}

Recently, a reverse Monte Carlo modeling³ based scheme was proposed⁴ for combining results of diffraction experiments (in the form of the primary information, the total scattering structure factor) and molecular dynamics (MD) computer simulations (using partial rdf's resulting from them). The approach was designed for allowing a quantitative assessment of the capabilities of a given interaction potential from the point of view of the structure. It was possible to establish in these early studies^{4,5} that out of two aqueous solutions of rubidium

bromide the MD-simulated structure of the 2 *m* (about 4 mol %) one showed much better consistency with neutron diffraction data than that of the concentrated (5 *m*, corresponding to about 10 mol %) solution. In an investigation of eight interaction potential models of water,⁶ the consistency between these potentials and the neutron diffraction data on heavy water⁷ was considered. It was found that while none of pair interaction models was perfect, most of them performed better than expected.

As the direct preliminary to the present investigations on aqueous cesium fluoride and cesium iodide solutions, a detailed, diffraction data based, MD-followed-by-RMC study (like in ref 4) was conducted on solutions of cesium chloride (CsCl)⁸ and cesium bromide (CsBr).⁹ Perhaps the most surprising finding of these works was, which contradicted with “common sense expectations” (as well as with results of refs 4 and 5), that it was not the ion–water but the water-related prdf's that could not be made consistent with diffraction results. This finding as well as the success in describing the liquid structure via this approach⁴

Received: February 17, 2012

Revised: July 13, 2012

Published: July 15, 2012

Table 1. Contributions of Partial Structure Factors to the Neutron- and X-ray-Weighted Total Scattering Structure Factors (Normalized, So That the Sum of the Contributions Equals Unity)^a

c/mol %	Cs–Cs	Cs–X	Cs–O	Cs–H	X–X	X–O	X–H	O–O	O–H	H–H
0.0 (N)								0.09	0.42	0.49
0.0 (X)								0.65; 0.92	0.31; 0.08	0.04; 0.00
CsF: 15 (N)	0.00	0.00	0.03	0.06	0.00	0.03	0.06	0.08	0.35	0.40
CsF: 15 (X)	0.20; 0.44	0.07; 0.07	0.34; 0.37	0.08; 0.01	0.01; 0.00	0.06; 0.03	0.02; 0.00	0.14; 0.08	0.07; 0.00	0.01; 0.00
CsF: 32 (N)	0.01	0.02	0.05	0.12	0.01	0.05	0.12	0.06	0.26	0.30
CsF: 32 (X)	0.41; 0.65	0.15; 0.11	0.25; 0.20	0.06; 0.00	0.01; 0.00	0.05; 0.02	0.01; 0.00	0.04; 0.02	0.02; 0.00	0.00; 0.00
CsI: 1 (N)	0.00	0.00	0.00	0.00	0.00	0.00	0.00	0.09	0.42	0.48
CsI: 1 (X)	0.00; 0.01	0.01; 0.02	0.07; 0.17	0.02; 0.00	0.00; 0.01	0.07; 0.16	0.02; 0.00	0.52; 0.60	0.26; 0.02	0.03; 0.00
CsI: 3.9 (N)	0.00	0.00	0.01	0.02	0.00	0.01	0.01	0.09	0.40	0.46
CsI: 3.9 (X)	0.02; 0.07	0.05; 0.13	0.17; 0.25	0.04; 0.00	0.02; 0.06	0.17; 0.24	0.04; 0.00	0.31; 0.23	0.15; 0.01	0.02; 0.00

^aFor X-ray diffraction, these weighting factors depend on the value of the scattering variable, Q , and therefore, contributions at two Q values, at 0.5 and 10 \AA^{-1} , are provided (separated by semicolons). Note that for neutron diffraction (but *not* for X-ray diffraction), the same weighting factors are valid for the partial radial distribution functions in r -space. For the sake of comparison, weighting factors for pure water are also given. N: neutron diffraction; X: X-ray diffraction.

prompted us to extend our investigations to the full set of diffraction data taken on Cs solutions.¹⁰

The solubility range of Cs solutions is extremely wide (saturated solution of CsF: 30.42 mol % at 291 K;¹¹ saturated solution of CsI: 4.88 mol % at 293 K¹¹). In our earlier publications aqueous solutions of two cesium salts with solubilities between the extrema, CsCl⁸ and CsBr,⁹ have been considered. In this work, we wished to examine the two other cesium halides, fluoride and iodide, which represent solubility extrema for cesium halide solutions; also, these solutions represent extrema in terms of the size of the anions. The difference between solubilities, unfortunately, would not allow comparison between salt solutions of equal concentrations over a wide concentration range; this drawback, we believe, is counterweighted by the fact that comparison between saturated solutions is provided.

We apply the scheme mentioned above⁴ for revealing the microscopic structure of the solutions. Diffraction data will be complemented with molecular dynamics simulation results, in order to provide detailed structural models, as a function of salt concentration, that are consistent with neutron and X-ray diffraction data and as close as possible to results of computer “experiments”. The advantage of such structures is that they are constructed by using all the available underlying physical observations. In addition, detailed information concerning the applicability of the particular set of pair potential parameters for describing the structure of the particular cesium halide solution at a particular concentration will be obtained. The major difference of our approach from another structural modeling scheme, the “empirical potential structure refinement” (EPSR) method,¹² which has been frequently applied to electrolyte solutions (see, e.g., ref 13), is that we do not adjust values for the potential parameters. Instead, we explore different available models for the solvent. Another difference from EPSR is that here molecular dynamics is made use for generating the starting configuration, as opposed to a Monte Carlo based scheme.

For a detailed reasoning as to why Cs salts are favorable, see ref 9. In short, cesium ions have 54 electrons, and therefore, the cation–oxygen contribution to the X-ray diffraction pattern is considerable even at low concentration (see Table 1). Cation–cation and cation–anion contributions are exceptionally high for X-ray diffraction at higher concentration values, whereas neutron diffraction data still contain (for deuterated samples) mostly O–D and D–D contributions. CsF dissolves partic-

ularly well in water at room temperature: a concentration of 32.3 mol % can be achieved. This means that the weight of cation–cation correlations is exceptionally high. (Concerning the hydration of Cs⁺ and X⁻ ions in other systems, references will be given while comparing results of the present study with previous findings, in section 3.)

In the present work, aqueous solutions of cesium fluoride (CsF) at 15.1 and 32.3 mol % (one Cs⁺ and one F⁻ ion per about 6 and 2 water molecules, respectively) and cesium iodide (CsI) at 1.0 and 3.9 mol % (one Cs⁺ and one I⁻ ion per about 100 and 25 water molecules, respectively) are considered. For both cesium salts, the higher concentration values quoted above represent the solubility limit. To give a visual idea about what these concentration differences mean, Figure 1 depicts the

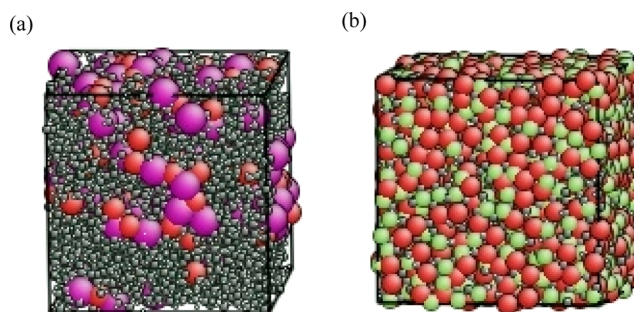


Figure 1. Snapshots taken from molecular dynamics simulation of (a) the 3.9 mol % CsI solution and (b) the 32.3 mol % CsF solution. Gray (small) balls: atoms of water molecules; red balls: Cs⁺ ions; magenta balls: I⁻ ions; light green balls: F⁻ ions. (Ball sizes are according to the van der Waals radii.) The pictures illustrate that although both solutions are at their saturated concentrations, the ion/water ratios are very different.

simulation boxes of the more concentrated solutions for both materials. While in the nearly saturated CsI solution ions are still quite rare, in the concentrated CsF solution it is the water molecules that are hardly visible.

In the next section experimental procedures are mentioned; computational details concerning molecular dynamics simulation and reverse Monte Carlo modeling are described in section 3. In section 4, results and their discussion are provided while section 5 summarizes our findings.

2. EXPERIMENTAL SECTION

Chemicals were purchased from Aldrich Chemical and were all of higher purity than 99%. The same, deuterated, solutions were applied for both neutron and X-ray diffraction experiments; this way, both the strong incoherent inelastic background of ^1H and any mismatch in terms of sample composition could be avoided.

Neutron diffraction measurements were carried out at room temperature and under atmospheric pressure, using standard 6 mm vanadium cans as sample holders. In case of CsF solutions, the PSD diffractometer installed at the Budapest Neutron Centre,¹⁴ whereas in case of CsI the SLAD diffractometer that used to operate at the Studsvik Neutron Research Laboratory¹⁵ have been utilized. The monochromatized neutron beam with a wavelength of about 1 Å allowed the measurement of the scattered intensity up to about 9.5 Å⁻¹ (PSD) to 10.5 Å⁻¹ (SLAD). Standard data corrections have been carried out using the CORRECT software package¹⁶ for CsI solutions, whereas in case of CsF solutions a program package developed specifically for the PSD diffractometer was utilized.¹⁷

X-ray diffraction experiments have been conducted at the SPring-8 synchrotron radiation facility (Japan), using the single-detector diffractometer setup of the BL04B2 (high-energy X-ray diffraction) beamline.¹⁸ For the current experiments the energy of X-rays was 61.6 keV, facilitating the easy access of a momentum transfer range up to about 16 Å⁻¹. Corrections to yield structure factors have been made by standard procedures, as described, for instance, in ref 19.

Total scattering structure factors for the case of neutron diffraction are defined throughout this work via the following equations (see, e.g., ref 20):

$$G^N(r) = \sum_{i,j=1}^n b_i b_j c_i c_j [g_{ij}(r) - 1] \quad (1a)$$

$$F^N(Q) = \rho_0 \int_0^\infty 4\pi r^2 G^N(r) \frac{\sin Qr}{Qr} dr \quad (1b)$$

In eqs 1a and 1b, c_i and b_i are the molar ratio and the scattering length of species i , $g_{ij}(r)$ are the partial radial distribution functions, $G^N(r)$ is the total radial distribution function, ρ_0 is the number density of the system, and Q is the scattering variable (proportional to the scattering angle); indexes i and j run through species of the system. For X-ray diffraction the quantity that takes the role of b_i , the so-called atomic form factor, $f_i(Q)$, depends on the value of the scattering variable Q and therefore, the composition of the X-ray-weighted tssf in reciprocal space has the form of

$$F^X(Q) = \sum_{i,j=1}^n f_i(Q) f_j(Q) c_i c_j [A_{ij}(Q) - 1] \quad (2)$$

where $A_{ij}(Q)$ are the partial structure factors that are Fourier transforms of the partial radial distribution functions $g_{ij}(r)$. Because of the Q -dependence of the weighting factors for X-ray diffraction, the Fourier transform of $F^X(Q)$, the X-ray weighted total radial distribution function, $G^X(r)$, can only be interpreted in a qualitative manner. For a precise evaluation of $F^X(Q)$ in real space, one needs to decompose it to partials in reciprocal space and take the Fourier transform of the partials to obtain the partial radial distribution functions, $g_{ij}(r)$. This procedure can only be realized via inverse methods, like RMC.

3. COMPUTATIONAL METHODS

3.1. Molecular Dynamics Simulation. We have carried out molecular dynamics simulations in the canonical (N,V,T) ensemble (with Berendsen thermostat²¹) using the GROMACS software.²² Following our earlier good experience on Cs halide solutions,^{8,9} the rigid and polarizable water model SWM4-DP²³ was selected. (We have actually tried other potentials, too, like SPC/E²⁴ and TIP4P-2005,²⁵ similarly to the case of CsBr;⁹ SWM4-DP proved to be the most favorable for CsF and CsI solutions. Details will be given in a separate publication.) Ionic interactions were mimicked by the S-type “Coulomb-plus-Lennard-Jones” parameter set.^{26–28} The pair potential energy function between the i th and the j th particles then took the following general form:

$$V_{ij}(r) = \frac{q_i q_j}{r_{ij}} + \frac{A_i A_j}{r_{ij}^{12}} - \frac{B_i B_j}{r_{ij}^6} \quad (3)$$

In eq 3 q_i are charges on the interaction sites, whereas A_i and B_i are the Lennard-Jones parameters (see ref 26 for Cs and refs 27 and 28 for F and I ions).

The number of particles and the density for each calculation can be found in Table 2.

Table 2. Some Parameters of the MD and RMC Calculations

	CsF 15.1 mol %	CsF 32.3 mol %	CsI 1 mol %	CsI 3.9 mol %
salt concn/mol %	15.07	32.29	1.00	3.91
number density/Å ⁻³	0.0872	0.0722	0.0996	0.0879
density/g cm ⁻³	1.94	2.74	1.24	1.45
no. of atoms (MD and RMC)	10001	9999	9999	9999
box length (MD and RMC; in Å)	48.59	51.73	46.48	48.45
max move (RMC; in Å)	0.1	0.1	0.1	0.1
units of (1 cation + 1 anion)/H ₂ O molecules	529/2981 = 0.1775	1206/2529 = 0.4769	33/3311 = 0.0100	132/3245 = 0.0407

3.2. Reverse Monte Carlo Modeling. Details of the reverse Monte Carlo method have been described in several publications.^{3,29–31} RMC is a simple tool for constructing large, three-dimensional structural models that are consistent with the total scattering structure factors (within the estimated level of their errors) obtained from diffraction experiments. For the present purpose the most attractive feature of the RMC method is that it can take any external information that can be calculated directly from the coordinates of the particles. Partial radial distribution functions from MD simulations are this type of information. If consistency with all input data is reached, then it may be stated that the different pieces of input data are consistent with each other as well as with the resulting particle configurations. On the other hand, if some of the input data cannot be approached within their uncertainties, then it means that parts of the input data set are not consistent with other pieces of input information. In our case this would mean that some of the input prdf's from MD would not be consistent with the experimental input total scattering structure factors. The resulting RMC particle configurations would still be consistent with experimental data and with some of the input prdf's. For the partial radial distribution functions the modeling background, the pair potential, is known. Thus, these configurations

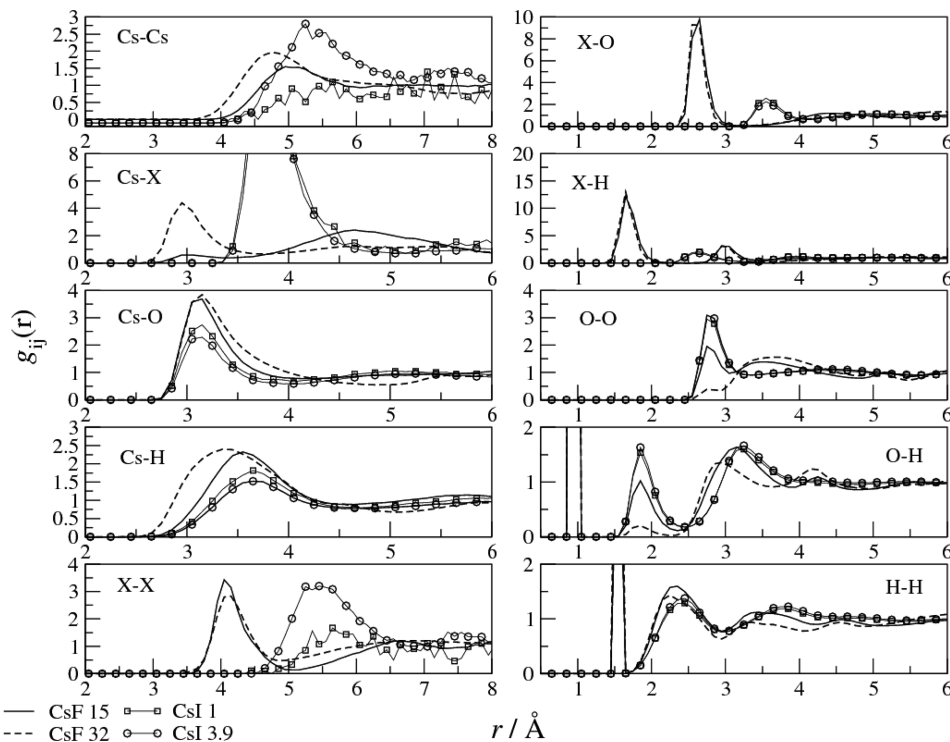


Figure 2. Partial radial distribution functions of CsF and CsI aqueous solutions, as obtained from molecular dynamics simulations. Solid lines: 15 mol % CsF; dashed lines: 32.3 mol % CsF; lines with empty squares: 1 mol % CsI; lines with empty circles: 3.9 mol % CsI.

would still represent enhanced structural models of aqueous CsF and CsI solutions, over a wide range of concentrations.

In the RMC calculations that are important ingredients of the present research the experimental data set consists of two total scattering structure factors: one from neutron and one from X-ray diffraction. “Real” experimental (diffraction) data were measured as described in section 2. The other, “quasi-experimental”, set of input information for RMC modeling, the set of simulated partial radial distribution functions, was provided by molecular dynamics simulations, as described in section 3.1. During the reverse Monte Carlo calculations that provided the structural models for further geometrical analysis, we required “perfect” agreement (within experimental uncertainties; for a more elaborated definition of “perfect”, see section 4) with diffraction data and wanted to see how many of the potential-based partial rdf’s could be fitted at the same time. The final set of prdf’s contained all the 10 $g_{ij}(r)$ ’s for the highly concentrated samples, whereas at the lowest concentration (1.0 mol % CsI solution) the three ion–ion prdf’s (Cs–Cs, Cs–I, and I–I) were not considered, for their insignificance and because of the poor statistics of even the MD-based prdf’s. (Note that the ion–ion prdf’s have a combined weight below 1% in the diffraction signals, and thus their omission does not represent any noticeable loss of information.) One more point must be mentioned here for clarity: the O–H and H–H prdf’s contain intramolecular contributions, and since these are just sharp “spikes” for a rigid water model (like SWM4-DP), the intramolecular regions are not considered during RMC modeling, which the latter technique operates by using flexible water molecules. Thus, the molecular geometry is influenced mainly by the experimental data in RMC.

Technical details (density, system size) of the RMC calculations are provided in Table 2. In each calculation, more than 1 million moves were accepted. This number may

seem to be somewhat low, about 100 accepted steps/atom; note, however, that RMC modeling has always been preceded by long, well-equilibrated MD simulations. This way, reverse Monte Carlo calculations may be considered as a “refinement” of the MD results. Many different runs were completed where both experimental and MD input were considered, with varying requirements concerning which data should be fitted closest; a common feature is that “perfect fit”, i.e., one with an uncertainty within the assumed level of errors, to experimental data has always been required.

4. RESULTS AND DISCUSSION

We begin with the basic structural results from MD simulations, the partial radial distribution functions, shown in Figure 2. A more detailed discussion of the curves will be provided below; for the moment, the most important observation in case of CsI is that hardly any concentration dependence can be detected, apart from the ion–ion partials. (Note that at a concentration of 1 mol % statistics for the like–like partials are bad and also that the curves are rather featureless, so that they will not be considered any further.) Differences between prdf’s of the two CsF solutions are significant, except for the anion–anion and anion–water relations. A most remarkable feature is that at extremely high (32.3 mol %) salt concentration oxygen and hydrogen atoms around the cation are located within almost the same distance. At the same concentration, regular H-bonded water–water arrangements are nearly entirely absent, as signified by the first (intermolecular) maxima of the O–O and O–H prdf’s; on the other hand, the first H–H coordination shell remains normal (i.e., similar to that observed at the lower concentration and in CsI solutions).

Figure 3 compares MD, RMC and experimental neutron- and X-ray-weighted total scattering structure factors at each concentration. “Goodness of fit” of the RMC calculations to

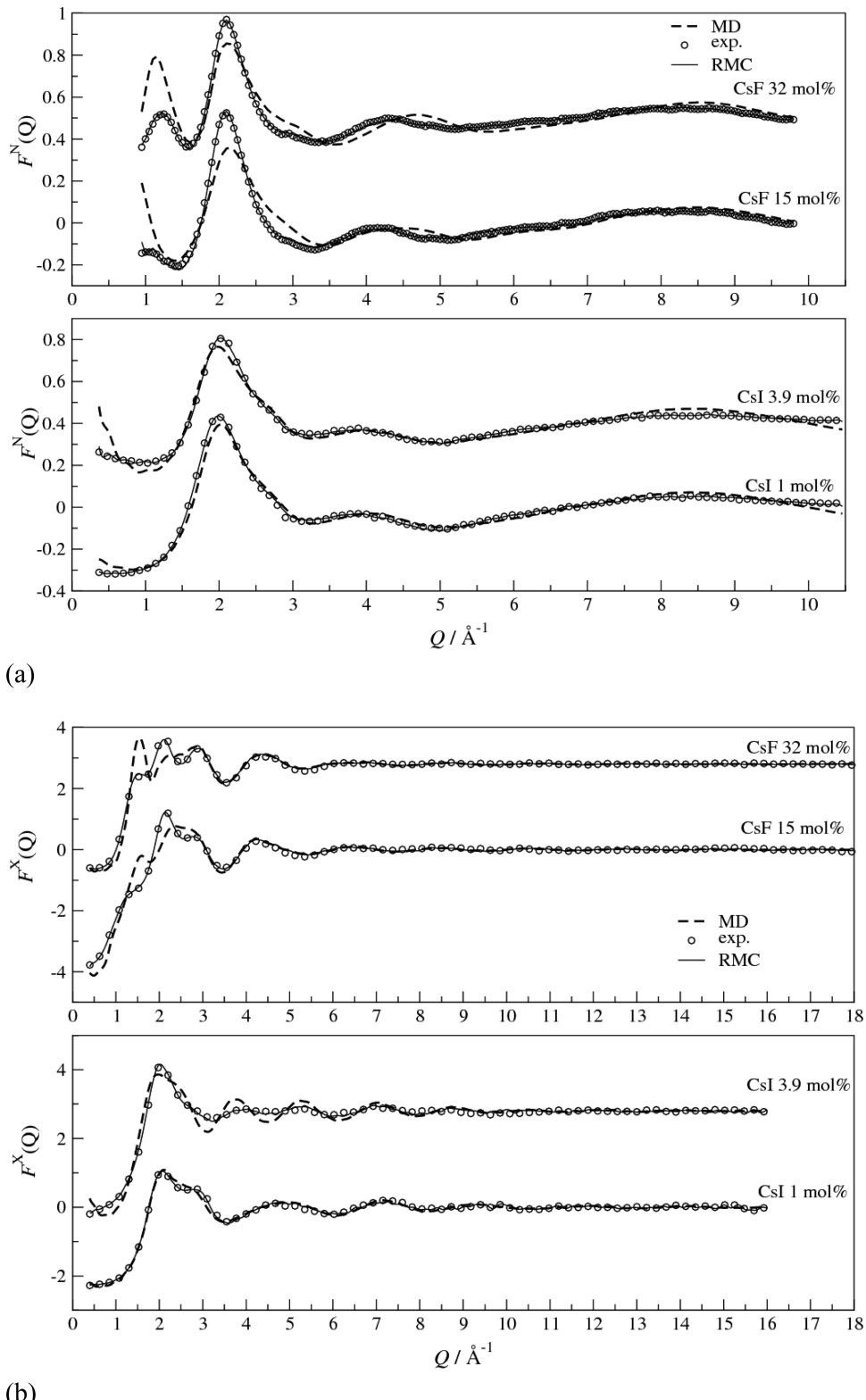


Figure 3. Total scattering structure factors from neutron (a) and X-ray (b) diffraction experiments (lines with empty symbols), together with RMC simulated tssf's with (solid line) and the corresponding curves as calculated from molecular dynamics simulations (dashed lines). Upper panels: CsF solutions; lower panels: CsI solutions.

experimental data is excellent; i.e., the particle configurations resulting from these two types of calculations are consistent with diffraction experiments within errors. It is now appropriate to mention the measure that characterize “goodness of fits”: throughout this work we use the “R-factor” (R_w) values as they

are well-known to crystallographers.³² R_w is essentially a normalized sum of squared differences between experimental and simulated tssf's; according to its common usage, a model structure factor is taken as satisfactory if R_w is less than 10%.³² Equation 4 provides the definition of the R_w factor that is used

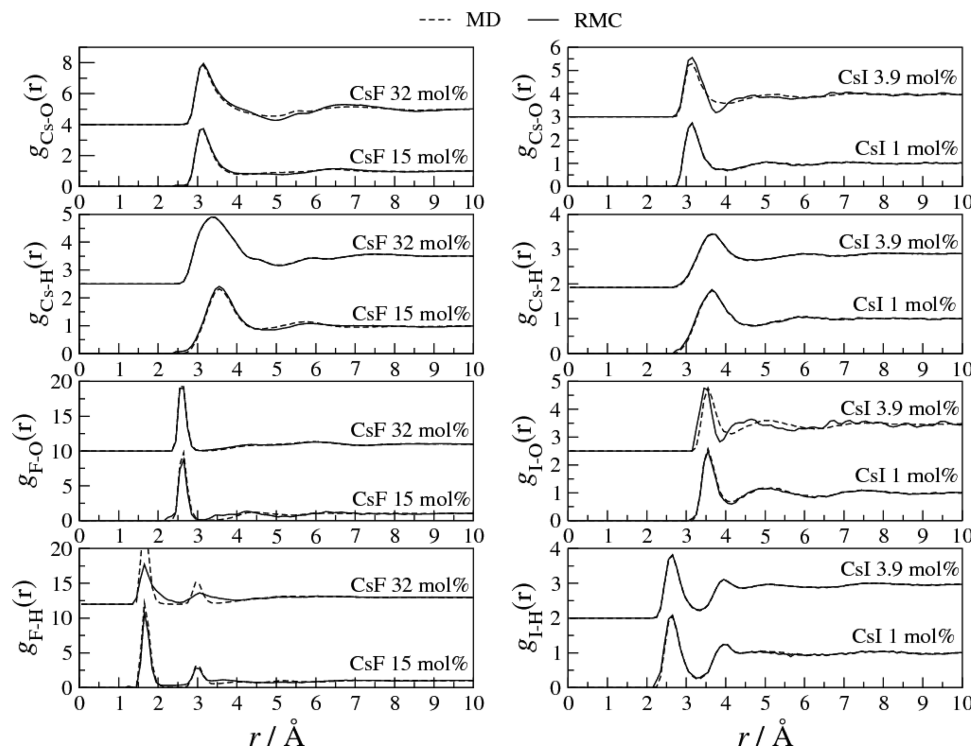


Figure 4. Partial radial distribution functions from RMC models (solid lines) and MD simulations (dashed lines) characterizing the solvation structure of ions at each concentration. Left panels: CsF solutions; right panels: CsI solutions.

in this work, as expressed for the case of a total scattering structure factor:

$$R_w^2[F(Q)] = \sum_i (F^C(Q_i) - F^E(Q_i))^2 / \sum_i F^E(Q_i)^2 \quad (4)$$

Indices “C” and “E” refer to “calculated” and “experimental” quantities, respectively.

For the present tssf’s, R_w has been between 3.4 and 6.7%, indicating convincing, but not suspiciously, close agreement. (For a comparison, we list here the prdf’s for which R_w was higher than 10%: I–O for the 3.9 mol % CsI solution, F–O for the 15 mol % CsF solution, and F–H for both CsF solutions.) “Perfect fit” will, from this point on, refer to fits to tssf’s for which R_w is well below 10%. Furthermore, although it cannot be proven rigorously, we suggest that these R_w values are actually useful indicators of the level of (systematic and statistical) errors of the measured and corrected tssf’s.

The overall agreement between MD and experiment is also rather encouraging: for instance, both neutron and X-ray diffraction data are reproduced at a nearly quantitative level for the 1 mol % CsI solution. For CsF solutions, on the other hand, MD results are less convincing: around the main peak, both X-ray and neutron-weighted tssf’s exhibit serious discrepancies as compared to diffraction data. (For fairness, it may be appropriate to mention that good general agreement to various structural data on the low concentration CsI solution indicates that the potential model is probably quite good for pure water; note that this observation does also carry useful information.) The level of inconsistencies increases with concentration for both CsI and CsF solutions. In addition, some neutron-weighted tssf’s calculated from MD configurations possess a clear small-angle scattering signal which is either missing from the corresponding experimental curve or the experimental

intensity is much lower. It is therefore clear that MD simulation results cannot be applied directly for describing the structure of concentrated aqueous solutions of CsF. On the other hand, for CsI solutions the applied potential parameter set (see section 3.1) ensures an at least semiquantitative consistency with diffraction data.

One more noteworthy feature is that the neutron-weighted tssf of the more concentrated solution of cesium fluoride exhibits a significant (pre)peak preceding the main peak, at about 1.2 \AA^{-1} . The underlying structural characteristics that bring about this feature are currently being examined; a thorough comparison with the case of concentrated aqueous CsCl solutions appears to be promising (cf. ref 8). Further investigations may also be justified by the fact that these “low- Q ” features are the ones that pair potentials cannot yet describe on their own.

Figure 4 demonstrates that most of the ion–water pair correlations derived from MD simulations may be made fully consistent with experimental data; the exceptions are the 32.3 mol % CsF solution where F–H and the 3.9 mol % CsI solution where I–O prdf derived from RMC differ considerably (among ion–water prdf’s, only for these cases the R_w factor³² is higher than 10%). Although the level of consistency between potentials and diffraction data is somewhat lower here, it may be stated that the present finding is consistent with that for CsCl and CsBr solutions.^{8,9} It should be remembered that in a similar (although much less detailed) study on rubidium bromide solutions^{4,5} ion–water prdf’s proved to be fully inconsistent with results of neutron diffraction experiments at high concentration. This controversy exposes the need for carrying out similar investigations in a systematic way, following with further alkali halide solutions and, of course, a possible new, extended study of rubidium halide solutions.

Table 3. Average Partial Coordination Numbers As Calculated from RMC Models^a

	CsF (15.1 mol %)	CsF (32.3 mol %)	CsI (1 mol %)	CsI (3.9 mol %)
$n_{\text{Cs}-\text{Cs}}$	2.94 (6.0 Å)	6.61 (5.8 Å)	0.18 (6.8 Å)	1.97 (6.8 Å)
$n_{\text{Cs}-\text{X}}$	0.24 (3.5 Å)	2.26 (3.7 Å)	0.7 (4.8 Å)	1.73 (4.8 Å)
$n_{\text{Cs}-\text{O}}$	8.03 (3.9 Å)	6.54 (3.9 Å)	6.73 (3.8 Å)	5.13 (3.8 Å)
$n_{\text{Cs}-\text{H}}$	21.83 (4.5 Å)	20.97 (5.0 Å)	24.59 (4.7 Å)	17.78 (4.6 Å)
$n_{\text{X}-\text{X}}$	1.89 (5.0 Å)	3.59 (4.9 Å)	0.73 (6.8 Å)	2.03 (6.8 Å)
$n_{\text{X}-\text{O}}$	5.34 (3.1 Å)	3.72 (3.0 Å)	6.22 (4.05 Å)	3.95 (3.9 Å)
$n_{\text{X}-\text{H}}$	4.96 (2.1 Å)	2.53 (2.0 Å)	6.55 (3.3 Å)	4.80 (3.3 Å)
$n_{\text{O}-\text{O}}$	1.64 (3.0 Å)	0.29 (3.0 Å)	4.88 (3.4 Å)	4.86 (3.4 Å)
$n_{\text{O}-\text{H}}$	3.05 (2.4 Å)	2.21 (2.4 Å)	3.98 (2.4 Å)	3.66 (2.4 Å)
$n_{\text{H}-\text{H}}$	5.29 (2.9 Å)	3.19 (2.9 Å)	6.26 (3.0 Å)	5.70 (3.0 Å)

^aThe upper boundary of the first coordination shell was set at the first minimum of the corresponding prdf (given in the table after the coordination numbers).

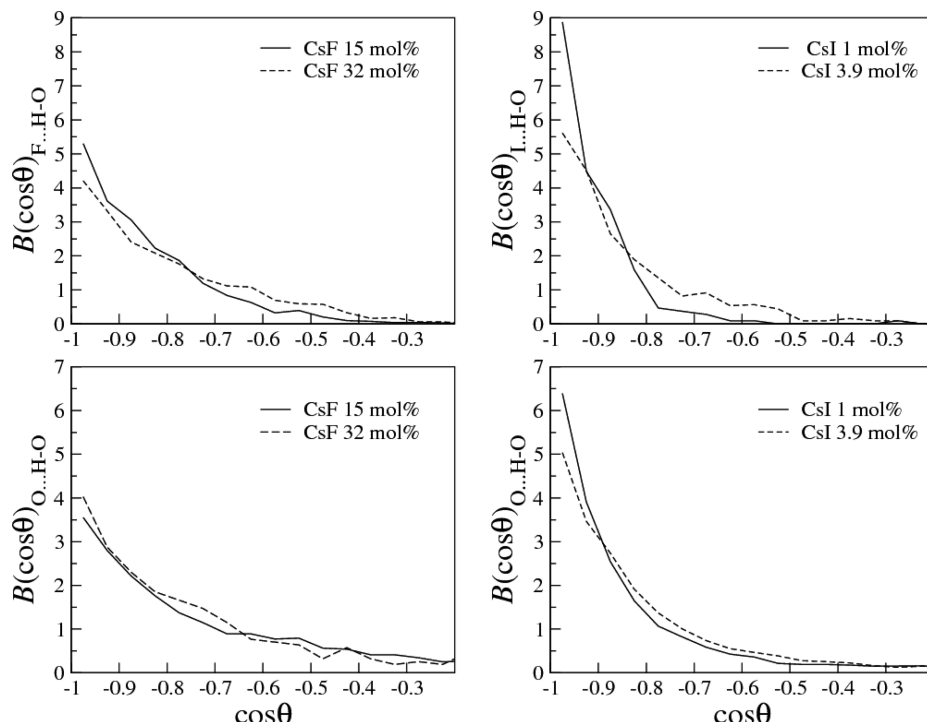


Figure 5. Distributions of cosines of X···H–O (X: F[−], I[−]) (upper panels) and O···H–O (lower panels) angles. Solid lines: lower concentrations; dashed lines: higher concentrations.

Concerning the hydration of the Cs⁺ cation, characteristics (peak position, peak height, peak width) of the first Cs–O and Cs–H peaks do not seem to change considerably either upon increasing the concentration (ref 7 reported a similar finding for CsCl solutions) or upon changing the counterion. Average coordination numbers around the Cs⁺ ion can be found in Table 3. With increasing concentration (and also, with increasing size of the anion) the number of the water molecules present in the hydration sphere of the cation decreases. Numerically, the average number of oxygen atoms in the first hydration sphere decreases from about 8.0 (15.1 mol %) to about 6.5 (32.3 mol %) in the case of CsF solutions and decreases from about 6.5 (1.0 mol %) to about 5 (3.9 mol %) in CsI solutions. It may be surprising that at (much) higher Cs⁺ concentration (in the CsF solutions) there are more O atoms around the ion. One explanation may be that in the 32.3 mol % CsF solution water molecules are “shared” among cations: the average number of cesium ions around an O atom is above 3. An alternative reasoning can be that iodide ions are much

bulkier than fluoride ions, and thus, if an iodide ion appears in the vicinity of a cesium cation, then simply a large volume is occupied so that there is less space remaining for water molecules. Concerning cesium iodide in water, these values are somewhat smaller than the value of 9.6 found for an infinitely dilute solution³³ and are in good agreement with the value of 7.9 found for a concentrated cesium iodide solution³⁴ by evaluating results of anomalous X-ray diffraction experiments. It may be noted, however, that the position of the Cs–O maximum was fixed at 3.0 Å in the latter work, whereas it appears between 3.1 and 3.2 Å here without any presumption. The number of H atoms found up to the first minimum of the Cs–H prdf is always much higher than 2 times the number of O atoms, which indicates that the boundaries of the Cs–O and Cs–H shells are not too well-defined; this behavior is similar to what was found earlier for CsCl solutions.⁸

The hydration shell of the fluoride ion is characterized by very well-defined F–O and F–H first maxima (see Figure 4). The positions and even the intensities (with the exception of

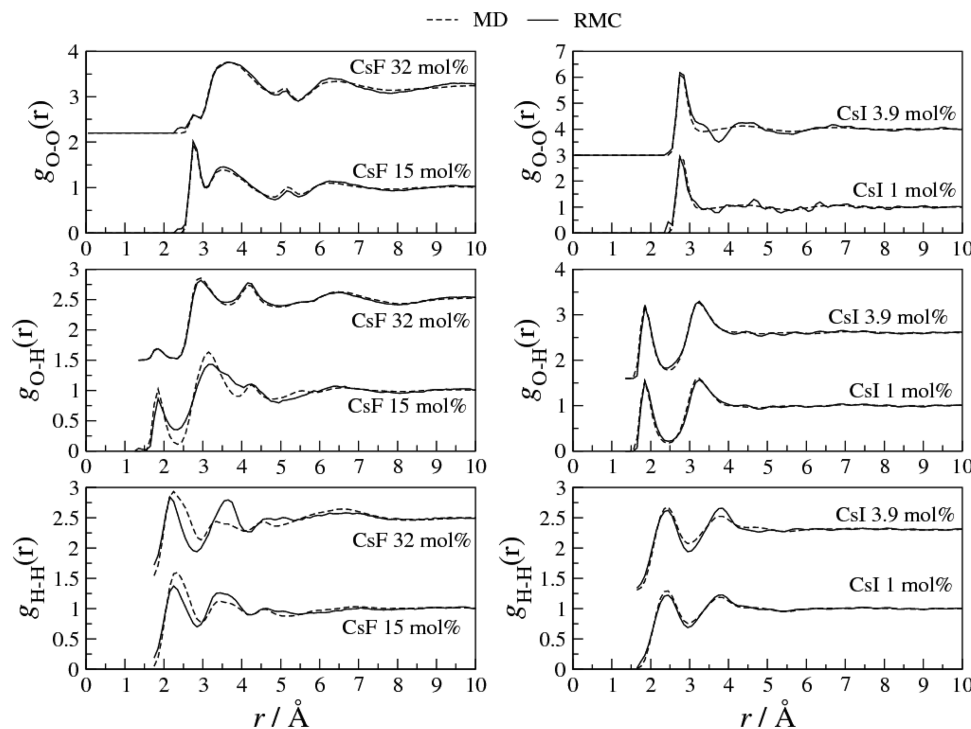


Figure 6. Partial radial distribution functions from RMC models (solid lines) and MD simulations (dashed lines) characterizing water–water correlations at each concentration. Top panels: O–O; middle panels: O–H; bottom panels: H–H. Left panels: CsF solutions; right panels: CsI solutions.

the F–H prdf of the 32 mol % CsF solution) are invariant under increasing concentration. The number of water molecules in the shell varies between 5.3 (15.1 mol %) and 3.7 (32.3 mol %). The average coordination number of both cations and anions are higher than the average number of water molecules/ion, so the hydration shells of the cations and anions must overlap.

It is worth noting that at the higher concentration the nearly solidlike pattern of the first two peaks cannot be made consistent with experimental data. This observation concerning the F–H/F–O prdf's may well be connected to the long existing discrepancy between computer simulations using classical^{33,35} and quantum mechanical³⁶ potential functions, namely, that classical potentials tend to suggest more water molecules around fluoride anions than quantum mechanical treatment do. On the basis of our present findings, which result from comparison with diffraction measurements, it is suggested that classical potentials overestimate the hydration number of the fluoride ion.

The hydration shell of the iodide ion is also characterized by a (perhaps, surprisingly) well-defined I–H first-neighbor distance at about 3.0 Å; the same value was obtained by Ramos et al.³⁴ The deep first minimum appears at about 3.5 Å. These characteristics do not change upon increasing concentration, although the number of H atoms in this neat shell decreases from about 6.6 to about 4.8 (see Table 3). The number of O atoms in the first I–O sphere at 1.0 mol % is equal to, whereas at 3.9 mol % it is somewhat higher than, the number of H atoms in the first I–H coordination sphere. That is, almost every O atom in the first shell has one H atom in between itself and the anion; i.e., the O–H bonds tend to point toward the anion.

The orientation of coordinated water molecules can be characterized by the distribution of the cosines of X···H–O

angles (see Figure 5, upper panels). These distributions are dominated by the presence of straight (180°) angles in each solution; the occurrence of such regular angles is most probable in the most dilute solution; that is, increasing the concentration of the salt distorts the anion hydration shell. These distortions are better visible for the larger counterion, even though the concentration difference between the two CsI solutions is smaller.

Water-related prdf's (Figure 6), especially O–H and H–H, appear to be the least consistent with the two experimental tssfs. (Note that only the intermolecular parts are fitted for the O–H and H–H prdf's, since the SWM4-DP water potential works with fixed molecular geometry.) By and large, the same was found for CsCl solutions.⁸ However, for CsF and CsI solutions, as it is demonstrated by Figure 6, the situation changes spectacularly as salt concentration grows. For the dilute solutions (i.e., solutions of CsI), nearly perfect agreement is found in terms of all the three “water–water” prdf's (O–O, O–H, and H–H); this indicates that at low and moderate Cs halide salt concentrations the SWM4-DP water potential model is able to produce a “water substructure” that is consistent with measured diffraction data. On the other hand, for (the more concentrated) CsF solutions the first intermolecular maximum of the H–H prdf's and the O–H prdf of the 15.1 mol % solution cannot be reproduced at the same level if agreement with diffraction data is required. This and our previous results for CsCl solutions (ref 8) indicate that for describing the structure of concentrated cesium halide solutions the water potential parameters are not entirely adequate.

The O–O prdf's (Figure 6, upper panels), as well as the O–O coordination numbers (Table 3), are in good agreement with the original MD results. There is only a small discrepancy on the O–O prdf of the 3.9 mol % CsI solution: MD predicts less structure than needed for reproducing experimental results. In

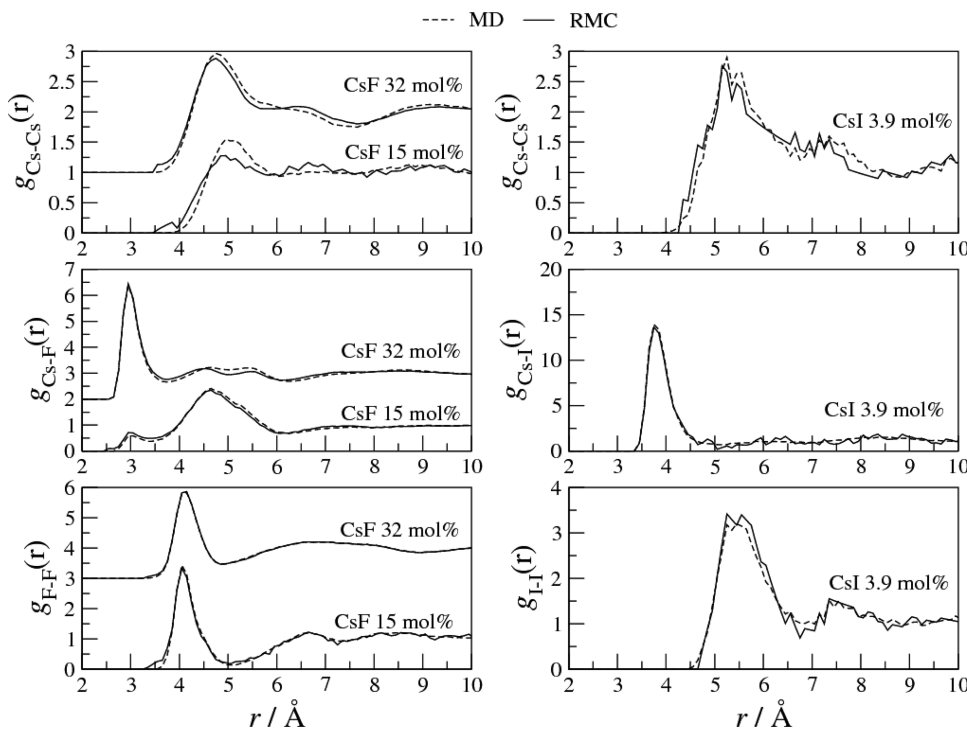


Figure 7. Partial radial distribution functions from RMC models (solid lines) and MD simulations (dashed lines) characterizing ion–ion correlations. Top panels: Cs–Cs; middle panels: Cs–X; bottom panels: X–X. (X: F, I) Left panels: CsF solutions; right panels: CsI solutions.

CsF solutions the average number of water molecules around a water molecule decreases from about 1.6 to about 0.3 as salt concentration increases from 15.1 to 32.3 mol %, as it can be devised from the O–O coordination number. The average number of H atoms around an O atom follows this change, although not so closely as it was in the case of CsCl and CsBr solutions:^{8,9} at the highest concentration, only 2.2 H atoms remain on average around an O atoms. This means that at the highest concentration most of the neighboring water molecules are not hydrogen bonded, since there cannot always be a H atom between two neighboring O atoms. In CsI solutions the number of oxygen atoms around oxygen atoms does not decrease noticeably with concentration; this is understandable as the number of water molecules/ion is rather high even close to saturation.

Finally, Figure 7 displays ion–ion partial radial distribution functions for the three solutions where these correlations contribute significantly to the measured structure factors (in the 1 mol % CsI solution there are too few ions for obtaining reliable results). Apart from visible discrepancies observed in the Cs–Cs prdf of the highly concentrated CsF solutions, prdf's provided by MD could be made consistent with diffraction data. By looking at Figures 4 and 7, it seems that counterions may appear in each other's first hydration shells. The number of counterions in the first hydration sphere of ions grows so that this growth almost exactly equals the loss of water molecules from the first coordination shell. That is, counterions do seem to replace water molecules, which phenomenon was also noticed for CsCl solutions.⁸ Contrary to earlier studies,^{34,37,38} we do not find genuine contact ion pairs in CsI solutions. This is partly due to the larger size of the iodide ions: they simply cannot get as close to the cation as the O atoms of water molecules. In the hydration shell of the cation (i.e., within the first minimum of the ion–oxygen distance) the average number of iodide ions is about 0.5; there are no counterions within the

first maximum of ion–oxygen distance. On the other hand, in CsF solutions 0.12 (15.1 mol %) and 1.25 (32.3 mol %) fluoride ions can be found around the cation within the first maximum of ion–oxygen distance. Contact $\text{Cs}^+ \cdots \text{F}^-$ ion pairs therefore do exist in the most concentrated solution of CsF.

5. CONCLUSIONS

We have investigated the structure of cesium fluoride and cesium iodide solutions in (heavy) water, over a wide range of salt concentrations, using the combination of neutron and X-ray diffraction experimental data with molecular dynamics simulations, via a reverse Monte Carlo based scheme. These salts represent extrema within cesium halide solutions, in terms of the size of the anion, as well as of the solubility in water: the smallest anion goes with the highest solubility (and vice versa). It has been established that, generally speaking, these extreme features do not exert extreme influence on the local structure.

By the analyses of particle configurations from reverse Monte Carlo models, we found the following characteristics of the structure of cesium fluoride and iodide solutions:

(1) The average number of water molecules around the Cs^+ cation decreases from about 8 to somewhat more than 5 as concentration and the size of counterion increase. At the very highest concentration (32.3 mol % of CsF), water molecules are shared by about 3 cesium cations on average.

(2) The average number of oxygen atoms in the first hydration sphere of anions decreases from about 5.3 (15.1 mol %) to about 3.7 (32.3 mol %) in case of CsF solutions, as it does from 6.2 (1.0 mol %) to about 4.0 (3.9 mol %) in CsI solutions. There is a strong preference toward nearly straight $\text{O}-\text{H}\cdots\text{F}^-$ and $\text{O}-\text{H}\cdots\text{I}^-$ (“hydrogen”-) bonds, regardless of the concentration or the anion.

(3) As concentration increases, counterions appear in the first coordination sphere of the ions in CsF solutions. Contact

$\text{Cs}^+ \cdots \text{F}^-$ ion pairs exist only in the most concentrated CsF solution; there, however, each ion participates in genuine pairs.

(4) At the highest salt concentration, hydrogen bonding between water molecules nearly ceases to exist. The H-bonding angle is getting systematically distorted as salt concentration grows.

Concerning the usefulness (and validity, as judged against diffraction data) of molecular dynamics results, it may be stated that the SWM4-DP polarizable water potential works surprisingly well for the solutions studied here, as only a couple of MD-based partial radial distribution functions proved to be inconsistent with diffraction data. Most of these difficult prdf's belong to water–water interactions; this finding is similar to the situation encountered while working with CsCl and CsBr solutions.

AUTHOR INFORMATION

Corresponding Author

*E-mail pusztai.laszlo@wigner.mta.hu; Fax +36 1 392 2589.

Notes

The authors declare no competing financial interest.

ACKNOWLEDGMENTS

We thank Mr. Anders Wannberg (Studsvik NFL, Sweden), Mr. György Mészáros (Wigner RCP, Hungary), and Dr. László Temleitner (Wigner RCP, Hungary) for their invaluable help with the neutron diffraction experiments. We thank the SPring-8 synchrotron facility (Hyogo, Japan) for providing beamtime for the X-ray diffraction experiments (instrument BL04B2, in the 2004A and 2007B periods; Proposal for the latter: 2007B1273). Financial support from the Hungarian National Research Fund (OTKA), through Grant K083529, is also acknowledged.

REFERENCES

- (1) See, e.g.: (a) Friedman, H. *Ionic Solution Theory, Based on Cluster Expansion Methods*; Interscience Publishers: New York, 1962. (b) Falkenhagen, H.; Ebeling, W.; Hertz, H. G. *Theorie der Elektrolyte*; S. Hirzel (Verlag): Leipzig, 1971. (c) Franks, F., Ed.; *Water, a Comprehensive Treatise*; Plenum Press: New York, 1973; Vol. 3. (d) Heinzinger, K. In Catlow, C. R. A., Parker, S. C., Allen, M. P., Eds.; *Computer Modelling of Fluids, Polymers and Solids*; Kluwer Academic Publishers: Dordrecht, 1990; p 357. (e) Bellissent-Funel, M.-C., Neilson, G. W., Eds.; *The Physics and Chemistry of Aqueous Ionic Solutions*; NATO ASI Series C; Reidel: Dordrecht, 1987; Vol. 205. (f) Barthel, J.; Krienke, H.; Kunz, W. *Physical Chemistry of Electrolyte Solutions: Modern Aspects*; Springer Verlag: Darmstadt, 1998.
- (2) Allen, M. P.; Tildesley, D. J. *Computer Simulation of Liquids*; Clarendon Press: Oxford, 1987.
- (3) McGreevy, R. L.; Pusztai, L. *Mol. Simul.* **1988**, *1*, 359.
- (4) Pusztai, L.; Harsányi, I.; Dominguez, H.; Pizio, O. *Chem. Phys. Lett.* **2008**, *457*, 96.
- (5) Pusztai, L.; Dominguez, H.; Pizio, O.; Sokolowski, S. *J. Mol. Liq.* **2009**, *147*, 52.
- (6) Pusztai, L.; Pizio, O.; Sokolowski, S. *J. Chem. Phys.* **2008**, *129*, 184103.
- (7) Soper, A. K. *J. Phys.: Condens. Matter* **2007**, *19*, 335206.
- (8) Mile, V.; Pusztai, L.; Dominguez, H.; Pizio, O. *J. Phys. Chem. B* **2009**, *113*, 10760.
- (9) Mile, V.; Gereben, O.; Kohara, S.; Pusztai, L. *J. Mol. Liq.* **2010**, *157*, 36.
- (10) Pusztai, L.; Harsányi, I.; Wannberg, A.; Kohara, S.; Sheptyakov, D. Private communication, 2009.
- (11) Chemical Book: <http://www.chemicalbook.com>.
- (12) (a) Soper, A. K. *Chem. Phys.* **1996**, *202*, 295. (b) Soper, A. K. *Phys. Rev. B* **2005**, *72*, 104204.
- (13) Soper, A. K.; Weckström, K. *Biophys. Chem.* **2006**, *124*, 180.
- (14) Sváb, E.; Mészáros, G.; Deák, F. *Mater. Sci. Forum* **1996**, *228*, 247.
- (15) Wannberg, A.; Mellergård, A.; Zetterström, P.; Grönros, M.; Karlsson, L.-E.; McGreevy, R. L. *J. Neutron Res.* **1999**, *8*, 13.
- (16) Howe, M. A.; McGreevy, R. L.; Howells, W. S. *J. Phys.: Condens. Matter* **1989**, *1*, 3433.
- (17) Mészáros, G.; Temleitner, L. Private communications, 2009.
- (18) Kohara, S.; Itou, M.; Suzuya, K.; Inamura, Y.; Sakurai, Y.; Ohishi, Y.; Takata, M. *J. Phys.: Condens. Matter* **2007**, *19*, 506101.
- (19) Kohara, S.; Suzuya, K.; Kashihara, Y.; Matsumoto, N.; Umesaki, N.; Sakai, I. *Nucl. Instrum. Methods, Sect. A* **2001**, *1030*, 467.
- (20) Keen, D. A. *J. Appl. Crystallogr.* **2001**, *34*, 172.
- (21) Berendsen, H. J. C.; Postma, J. P. M.; van Gunsteren, W. F.; DiNola, A.; Haak, J. R. *J. Chem. Phys.* **1984**, *81*, 3684.
- (22) <http://www.gromacs.org>. See also: Hess, B.; Kutzner, C.; van der Spoel, D.; Lindahl, E. *J. Chem. Theory Comput.* **2008**, *4*, 435.
- (23) Lamoureux, G.; Harder, E.; Vorobyov, I. V.; Roux, B.; MacKerell, A. D., Jr. *Chem. Phys. Lett.* **2006**, *418*, 245.
- (24) Berendsen, H. J. C.; Grigera, J. R.; Straatsma, T. P. *J. Phys. Chem.* **1987**, *91*, 6269.
- (25) Abascal, J. L. F.; Vega, C. *J. Chem. Phys.* **2005**, *123*, 234505.
- (26) Aqvist, J. *J. Phys. Chem.* **1990**, *94*, 8021.
- (27) Chandrasekhar, J.; Spellmeyer, D. C.; Jorgensen, W. *J. Am. Chem. Soc.* **1984**, *106*, 903.
- (28) McDonald, N. A.; Duffy, E. M.; Jorgensen, W. *J. Am. Chem. Soc.* **1998**, *120*, 5104.
- (29) McGreevy, R. L. *J. Phys.: Condens. Matter* **2001**, *13*, R843.
- (30) Evrard, G.; Pusztai, L. *J. Phys.: Condens. Matter* **2005**, *17*, S1.
- (31) Gereben, O.; Jóvári, P.; Temleitner, L.; Pusztai, L. *J. Optoelectron. Adv. Mater.* **2007**, *9*, 3021.
- (32) (a) McCusker, L. B.; von Dreele, R. B.; Cox, D. E.; Louer, D.; Scardi, P. *J. Appl. Crystallogr.* **1992**, *32*, 36. (b) Brünger, A. T. *Nature* **1992**, *355*, 472. (c) Online Dictionary of Crystallography, http://reference.iucr.org/dictionary/R_factor (last viewed: 25 May 2012).
- (33) Lee, S. H.; Rasaiah, J. C. *J. Phys. Chem.* **1996**, *100*, 1420.
- (34) Ramos, S.; Neilson, G. W.; Barnes, A. C.; Buchanan, P. *J. Chem. Phys.* **2005**, *123*, 214501.
- (35) (a) Laudernet, Y.; Cartailler, T.; Turq, P.; Ferrario, M. *J. Phys. Chem. B* **2003**, *107*, 2354. (b) Koneshan, S.; Rasaiah, J. C.; Lynden-Bell, R. M.; Lee, S. H. *J. Phys. Chem. B* **1998**, *102*, 4193.
- (36) (a) Ohrn, A.; Karlstrom, G. *J. Phys. Chem. B* **2004**, *108*, 8452. (b) Ho, M. H.; Klein, M. L.; Kuo, I. F. W. *J. Phys. Chem. A* **2009**, *113*, 2070. (c) Heuft, J. M.; Meijer, E. J. *J. Chem. Phys.* **2005**, *122*, 7.
- (37) Lawrence, R. M.; Kruh, R. F. *J. Chem. Phys.* **1967**, *47*, 4758.
- (38) Tamura, Y.; Yamaguchi, T.; Okada, I.; Ohtaki, H. Z. *Naturforsch., A: Phys. Sci.* **1987**, *42A*, 367.